International Immunopharmacology 99 (2021) 107975

Contents lists available at ScienceDirect

International Immunopharmacology

journal homepage: www.elsevier.com/locate/intimp

Astrocyte-derived CCL7 promotes microglia-mediated inflammation following traumatic brain injury

Jianqin Xue [a], Yu Zhang [a], Junhua Zhang [b], Zhujun Zhu [a], Qi Lv [a], Jianhua Su [b,*]

[a] Department of Rehabilitation Medicine, Jintan Hospital affiliated to Jiangsu University, Changzhou 213200, China
[b] Neurology Department, Jintan Hospital affiliated to Jiangsu University, Changzhou 213200, China

ARTICLE INFO

Keywords:
Traumatic brain injury
CCL7
Inflammation
Microglia
Astrocytes

ABSTRACT

Microglia are immune cells of the central nervous system that mediate neuroinflammation. It is widely known that microglia-mediated inflammation in the brain contribute to the widespread tissue damage and neurological deficits in traumatic brain injury (TBI). However, the mechanisms responsible for this inflammatory response remain elusive. Here, we investigated the role of astrocyte-derived chemokine (C-C motif) ligand 7 (CCL7) in microglial-controlled inflammation following TBI. Our results demonstrated that astrocyte-derived CCL7 induced microglial activation and the release of proinflammatory mediators in the cortex and serum of rats that underwent experimental TBI. Furthermore, CCL7 knockout improved microglia-controlled inflammation, brain morphology and neurological dysfunction following TBI. In vitro, CCL7-siRNA attenuated the LPS-induced expression of pro-inflammatory markers in the co-culture of microglia and astrocytes. Collectively, our findings uncover an important role for astrocyte-derived CCL7 in promoting microglia-mediated inflammation after TBI and suggests CCL7 could serve as a potential therapeutic strategy for attenuating TBI by inhibiting microglial activation.

1. Introduction

Traumatic brain injury is a head injury typically triggered by an external force that results in severe physical, psychological, and cognitive impairments [1]. As a leading cause of death and disability around the globe, TBI represents a critical public health and socio-economic problem [2]. It is estimated that over 50 million new TBI cases occur annually, and TBI survivors have a pooled standardized mortality ratio [3]. Nevertheless, few clinical treatments have been shown to convincingly reverse the pathology and long-term functional deficits after human TBI, emphasizing the need for studies that reveal the precise mechanisms of TBI.

Traumatic brain injury (TBI) causes cell death and neurologic dysfunction through secondary injury mechanisms including glial activation, inflammation, free radical generation, and glutamate excitotoxicity [4]. It has been reported that the injury-induced inflammatory response significantly contributes to the progression of secondary injury and impact post-injury recovery [5]. Moreover, therapies alleviating the inflammatory reaction were shown to improve TBI damage [6]. Microglia are the resident immune cells that express a variety of pattern recognition receptors (PRRs) at their cell surface and intracellularly, allowing them to mount an immune response [7]. The inflammatory response to TBI is highly complex and associated with microglial activation and further release of multiple proinflammatory mediators [8].

Chemokines are small secreted proteins that control the migration and positioning of immune cells in tissues and are essential for the function of the immune system [9]. CCL2 and CCR2 are two common activators of microglia that are mainly detected in microglia in mouse and human brains [10,11]. Chemokine (C-C motif) ligand 7 (CCL7, also known as MCP-3) is a chemotactic factor and potent attractant of monocytes that can bind and signal via multiple CC chemokine receptors including CCR2 [12]. CCL7 can be secreted by astrocytes, the most abundant cell type in the mammalian brain [13–15]. Traumatic brain injury is a disease associated with reactive astrogliosis [16]. Although existing evidence suggests that astrocyte-released CCL7 is a powerful mediator involved in the inflammatory response under pathological conditions, little is known about their function in microglia-mediated inflammation after traumatic brain injury [11].

In this study, we used an in vivo TBI model to investigate the effect of astrocyte-derived CCL7 on microglia-mediated inflammation. Furthermore, the role of CCL7 in microglia-related inflammatory action following TBI was explored using CCL7 knockout (KO) mice ($CCL7^{-/-}$).

* Corresponding author at: 500 Jintan Avenue, Jintan District, Changzhou 213200, China.
E-mail address: 1000004299@ujs.edu.cn (J. Su).

https://doi.org/10.1016/j.intimp.2021.107975
Received 7 January 2021; Received in revised form 24 June 2021; Accepted 8 July 2021
Available online 19 July 2021

a

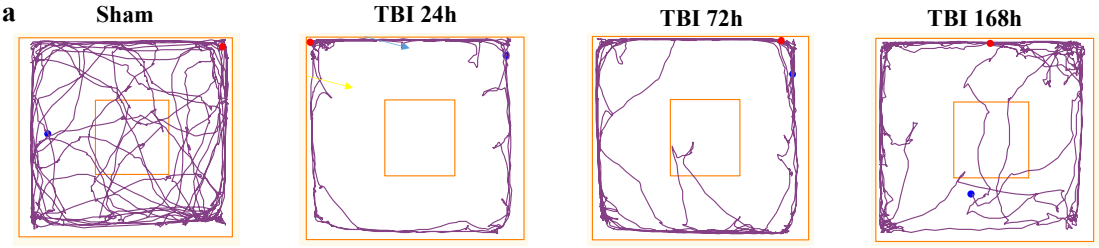

b

	Sham	TBI 24h	TBI 72h	TBI 168h
Total distance (mm)	26.26±2.187	15.47±1.851**	17.10±1.666**	22.21±1.523
Time in center (s)	64.65±4.069	10.89±1.205**	17.75±1.460**	28.18±2.002**
Discrimination index (%)	0.7948±0.03614	0.2823±0.05150**	0.2271±0.02637**	0.3688±0.02221**
mNSS score	0.500±0.1890	7.750±0.4119**	5.250±0.5590**	2.875±0.2266**

Fig. 1. Neurological deficits following TBI. (a) Spontaneous locomotor activity and anxiety-like behavior were assessed using the OFT test. (b) TBI caused a decrease in total distance and time in center in the OFT. Meanwhile, mice underwent TBI had lower discrimination indexes in the NOR and higher mNSS scores in mNSS evaluation. Data are presented as mean ± SEM (n = 8–10 per group). ** $p < 0.01$, compared to Sham group.

a

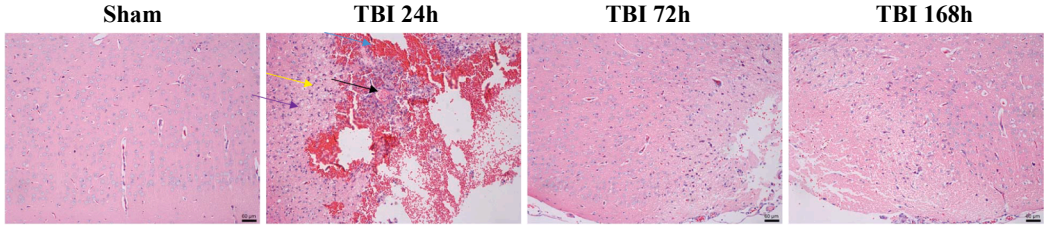

b

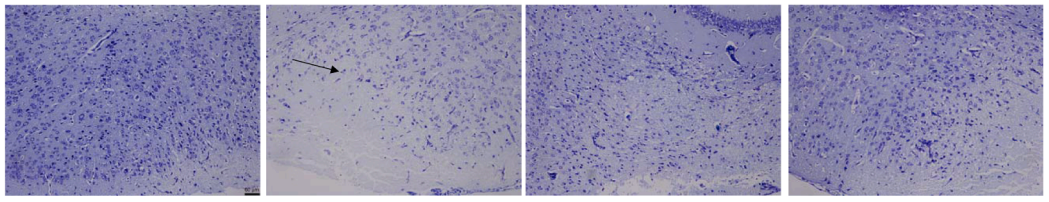

c

	Sham	TBI 24h	TBI 72h	TBI 168h
Number of cells/mm^2	124.3±8.988	29.33±3.756**	59.00±4.619**	76.33±6.741**
Brain water content (%)	75.13±0.2827	85.21±0.4017**	86.41±0.6339**	83.24±0.3633**

Fig. 2. Pathological changes following TBI. (a) Representative 60 × H&E microphotographs depicting the ipsilateral cortex in the four study groups. Heavy bleeding (blue arrow), eosinophil accumulation (black arrow), increased glial cells (purple arrow), irregular shape and pyknotic and deeply stained neurons (yellow arrow) were prominent in area surrounding the lesion following TBI. (b) Images of the *peri*-impact area in the cortex. Arrow indicates Nissl body. Scale bar = 60 μm. (c) Quantitative analysis of Nissl bodies and brain water content in the injured cortex. Data are presented as mean ± SEM (n = 4–6 per group). ** $p < 0.01$, compared to Sham group.

2. Materials and methods

2.1. Animals

Male C57BL/6 mice were purchased from China Academy of Military Medical Sciences (Beijing, China). CCL7$^{-/-}$ mice (on a C57BL/6J background) were provided by GemPharmatech Co., Ltd. (Nanjing, China). Animals were housed in an animal facility (22-24 °C) under a 12-hour light–dark cycle with ad libitum access to food and water. All procedures were conducted in accordance with the Provision and General Recommendation of Chinese Experimental Animals Administration Legislation.

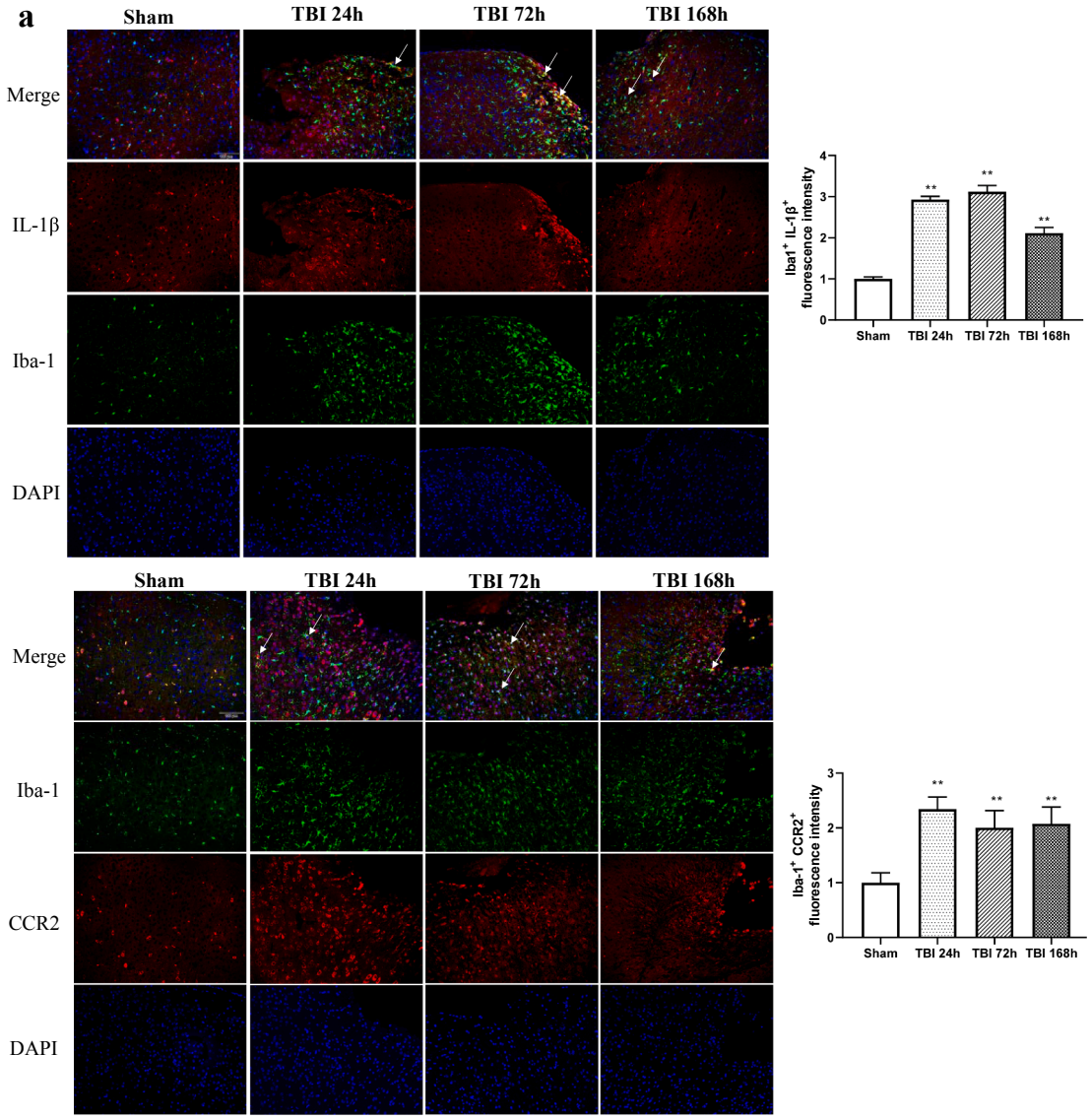

b

		Sham	TBI 24h	TBI 72h	TBI 168h
Cortex (pg/mg)	TNF-α	5.367±0.4111	7.963±0.3560**	8.595±0.4281**	7.492±0.3278**
	IL-1β	2.333±0.4282	5.413±0.5718**	7.283±0.6977**	6.150±0.3695**
	IL-6	10.00±1.388	18.93±1.106**	22.09±1.684**	18.91±1.349**
	IL-18	24.29±0.9715	38.99±2.523**	41.91±2.305**	38.81±1.770**
Serum (pg/mL)	TNF-α	74.66±7.008	97.79±8.727**	141.6±4.375**	170.6±6.822**
	IL-1β	36.79±2.405	58.08±4.089**	77.81±3.843**	60.26±5.587**
	IL-6	24.84±2.816	48.97±2.385**	48.16±2.736**	42.70±2.964**
	IL-18	36.04±2.487	57.41±2.546**	62.91±2.969**	54.10±3.639**

Fig. 3. Iba-1 immunoreactivity and pro-inflammatory cytokine levels following TBI. (a-b) Co-localization of CCL7 Iba-1 (a microglia-specific marker) with IL-1β and CCR2 on TBI brain sections (n = 3 per group). Scale bar = 100 μm. (c) Levels of TNF-α, IL-1β, IL-6 and IL-18 in the cortex and serum were measured by ELISA. TBI caused a significant increase in the concentrations of TNF-α, IL-1β, IL-6 and IL-18 in the cortex and serum (n = 6 per group). Data are presented as mean ± SEM. ** $p < 0.01$, compared to Sham group.

2.2. Experimental design

To assess the influence of CCL7 on microglia-mediated inflammation in TBI, the study consisted of two experiments, both of which used the same CCI protocol.

Experiment 1: Forty-eight male C57BL/6 mice were randomly divided into four groups (n = 12/group): sham, TBI 24 h, TBI 72 h, TBI 168 group. TBI mice were exposed to CCI, while sham animals

a

	Sham	TBI 24h	TBI 72h	TBI 168h
Cortex CCL2 (pg/mg)	22.84±3.573	39.82±2.673**	38.80±5.708*	45.03±4.338*
Serum CCL2 (pg/mL)	123.4±6.790	202.5±16.87**	229.6±18.04**	243.9±19.74**

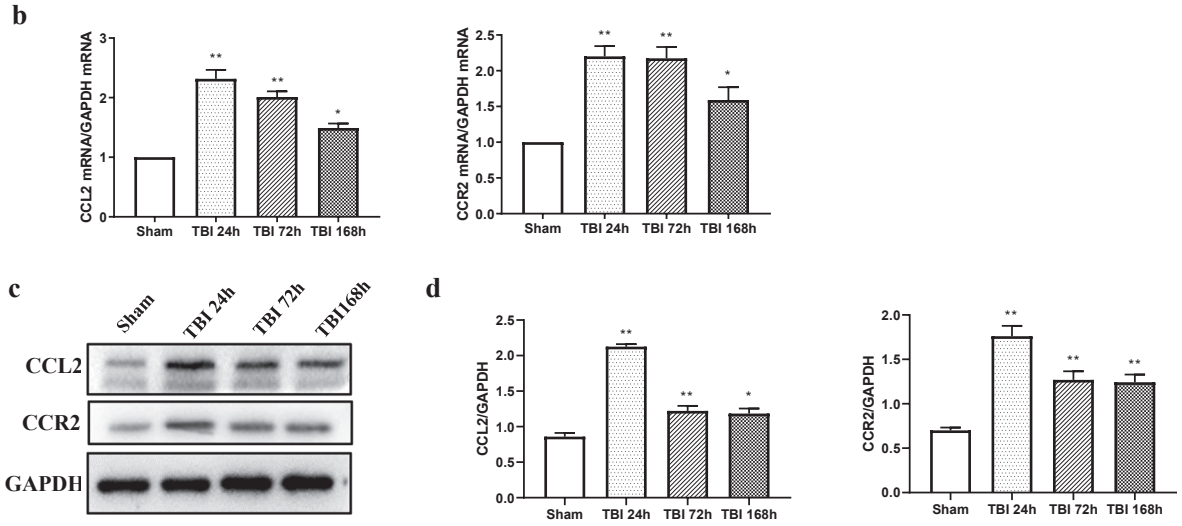

Fig. 4. CCL2 and CCR2 expression in the cortex and serum following TBI. (a) The ELISA analysis of CCL2 in the cortex and serum of mice (n = 6 per group). (b) The mRNA expression of CCL2 and CCR2 in the cortex was measured by real time RT-PCR (n = 3 per group). (c) The protein expression of CCL2 and CCR2 in the cortex was detected by western blot (n = 3 per group). Data are presented as mean ± SEM. * $p < 0.05$, ** $p < 0.01$, compared to Sham group.

underwent the same procedure except for the contusion. At the indicated time point, behavioral tests including neurological severity score (mNSS) evaluation, open field test (OFT) and novel object recognition test (NOR) were performed sequentially to evaluate the neurological deficits of mice. Then blood was collected, and animals were euthanized by cervical dislocation.

Experiment 2: Twenty-four male CCL7 wild type and twenty-four CCL7 knockout ($CCL7^{-/-}$) mice were randomly assigned to either a sham group or a TBI group (n = 12 per group). TBI mice were exposed to CCI, while sham animals underwent all surgical procedures but were not subjected to the contusion. At 72 h post TBI, behavioral tests including mNSS, OFT and NOR were performed sequentially to evaluate the neurological deficits of mice. Then blood was collected, and animals were euthanized by cervical dislocation.

2.3. Controlled cortical impact (CCI) injury

Traumatic brain injury was induced by controlled cortical impact as previously described [17]. Briefly, mice were anesthetized with isoflurane (induction: 3%, maintenance: 1.5%) and placed on a stereotaxic frame. A 5 mm craniotomy was performed to the left of the midline sagittal suture, between lambda and bregma. Then TBI mice received a single impact at 1.0 mm depth with a 3.5 mm diameter tip onto the cortex (6 m/s, Leica Biosystems). The sham mice received all procedures except the contusion.

2.4. Cell culture and treatment

Primary astrocytes were cultured from the cerebral cortices of 1-day-old C57/B6J mouse pups as described previously [18]. Briefly, the cerebral cortices were dissected out and the tissues were digested using 0.25% trypsin for 10 min at 37 °C. Subsequently, cells were seeded and maintained in Dulbecco's Modified Eagle Medium (DMEM)/F12 containing 15% FBS and penicillin/streptomycin. Cell suspensions were plated into 75 cm^2 flasks and incubated at 37 °C in a CO2 incubator (5% CO2). A week later, microglia and oligodendrocytes were removed by shaking for 16 h at 200 rpm. The resulting astrocytes were trypsinized, seeded into new flasks, and cultured for 6 days. Cell culture medium was changed twice a week. The confirmation of astrocytes was performed by immunofluorescence staining for the astrocytic marker GFAP. For knockdown of CCL7, lentiviral infection was performed with astrocytes as described below. Forty-eight hours later, co-cultures of astrocytes and microglia were reconstituted by adding BV2 cells into astrocyte cultures [19]. Then, the mixed cultures were challenged with 1 μg/ml of LPS (Sigma, L2630, serotype O111:B4) for 6 h.

2.5. Lentiviral infection

For the inhibition of CCL7 expression using siRNA, primary mouse glial cells were grown to 80% confluence and transiently transfected with 50 nm CCL7 siRNA or the negative control (NC) siRNA for 48 h at 37 °C using Lipofectamine® 2000 reagent. CCL7 siRNA (forward 5′-GCCCAATGCATCCACATGCTGCTATTT-3′ and reverse 5′-ATAGCAGCATGTGGATGCATTGGGCTT-3′) and negative control siRNA were purchased from Bai Wo Rui Pharmaceutical Research Institute Co., Ltd. (Nanjing, China).

2.6. Open field test (OFT)

Mice were gently placed in the center of an open field apparatus (40 cm × 40 cm × 40 cm) and video recorded for 5 min. The total distance traveled and time spent in the central section (15 × 15 cm) were analyzed by ANY-maze software. The apparatus was cleaned with 70% alcohol between trials.

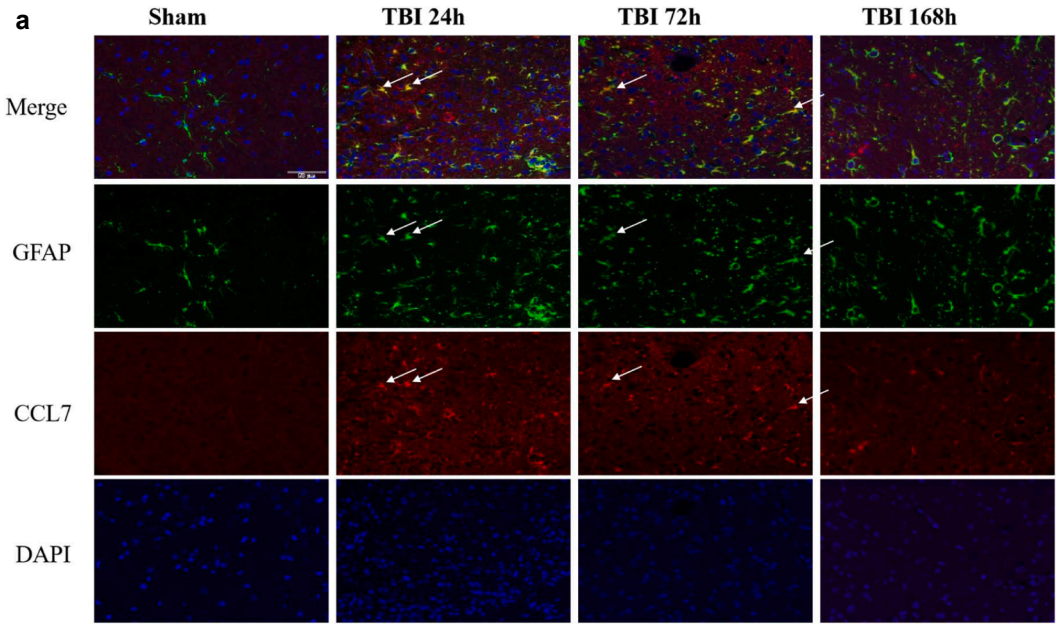

	Sham	TBI 24h	TBI 72h	TBI 168h
GFAP⁺cells/mm²	820.3±64.18	1267±78.31**	1263±57.16**	1204±67.43**
CCL7⁺ GFAP⁺ fluorescence intensity	732.7±131.1	8753±593.9**	6542±1003**	5549±605.6**

b

	Sham	TBI 24h	TBI 72h	TBI 168h
Cortex CCL7 (pg/mg)	13.66±1.076	20.82±0.9605**	25.27±1.740**	15.55±0.7439
Serum CCL7 (pg/mL)	81.53±6.055	179.7±13.00**	198.6±11.33**	216.3±11.71**

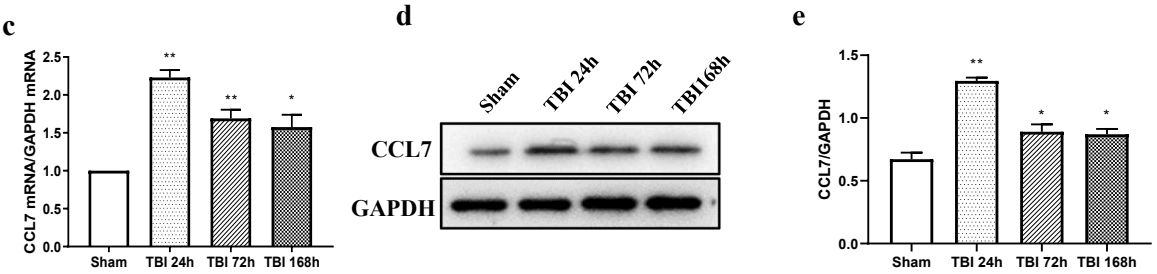

Fig. 5. CCL7 levels in the cortex and serum following TBI. (a) Co-localization of CCL7 and GFAP (an astrocyte-specific marker) on TBI brain sections (n = 3 per group). Quantification of GFAP + cells per area (mm^2) and $CCL7^+$ $GFAP^+$ fluorescence intensity. (b) The ELISA analysis of CCL7 in the cortex and serum of mice (n = 6 per group). (c) The mRNA expression of CCL7 in the cortex was measured by real time RT-PCR (n = 3 per group). (d-e) The protein expression of CCL7 in the cortex was detected by western blot (n = 3 per group). Data are presented as mean ± SEM. * $p < 0.05$, ** $p < 0.01$, compared to sham group.

2.7. Novel object recognition test (NOR)

The NOR test was performed as previously reported [20]. The mouse was placed in a white plexiglass box (40 cm × 25 cm × 20 cm) and exposed to two of the same objects for 10 min. One hour later, the mouse was returned to the box, and one of the familiar objects was replaced by a novel object. Mice were allowed to explored for 5 min and discrimination index was analyzed by ANY-maze software. The discrimination index was defined as (time spent exploring the novel object)/(total time spent exploring both objects)] × 100%.

2.8. Assessment of neurological function

To evaluate the neurological functional deficit, the modified neurological severity score (mNSS) which includes motor, sensory, balance, and reflex tests was performed [21]. The mNSS score was graded on a

a

	Wild type+Sham	Wild type+TBI	CCL7$^{-/-}$+Sham	CCL7$^{-/-}$+TBI
Total distance (mm)	24.06±1.941	13.51±0.8141$^{\#\#}$	26.11±2.042	19.57±1.213$^{\&}$
Time in center (s)	56.13±1.650	11.31±1.204$^{\#\#}$	58.23±2.736	26.92±1.451$^{\&\&}$
Discrimination index (%)	85.37±3.073	30.90±4.576$^{\#\#}$	89.14±3.038	52.45±2.301$^{\&\&}$
mNSS score	0.7000±0.1528	6.700±0.3958$^{\#\#}$	0.5000±0.1667	5.400±0.3399$^{\&}$

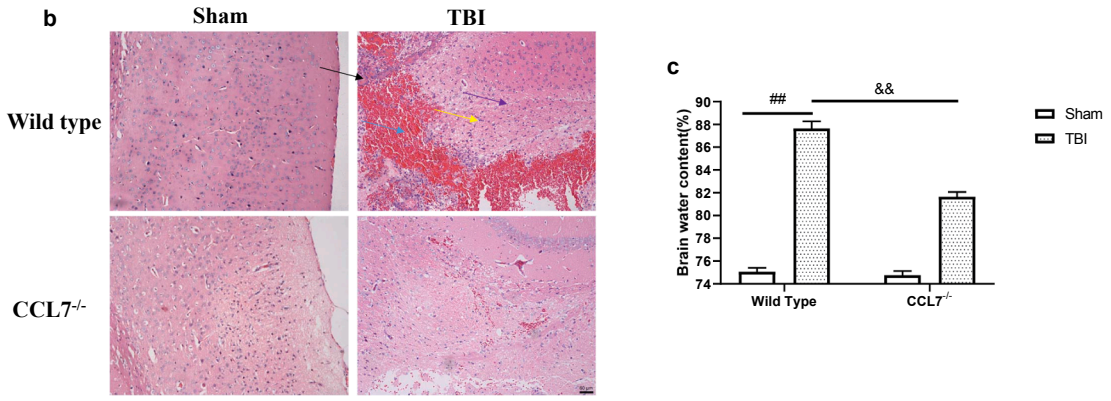

Fig. 6. Effects of CCL7 deletion on TBI-induced neurological deficits and pathological changes. (a) CCL7 deletion reversed TBI-induced increase in mNSS scores as well as decrease in discrimination index, total distance and time spent in center (n = 10 per group). (b) Representative 60 × H&E microphotographs depicting the ipsilateral cortex in the four study groups. Heavy bleeding (blue arrow), eosinophil accumulation (black arrow), increased glial cells (purple arrow), irregular shape and pyknotic and deeply stained neurons (yellow arrow) were prominent in area surrounding the lesion following TBI. (c) Quantitative analysis of brain water content (n = 3 per group). Data are presented as mean ± SEM. Statistical analysis: two-way ANOVA followed by Tukey correction. $^{\#\#}$ $p < 0.01$, compared to wild type + sham group; $^{\&}$ $p < 0.05$, $^{\&\&}$ $p < 0.01$, compared to wild type + TBI group.

scale of 0–18 (0 = normal function; 18 = maximal deficit). The test was conducted by investigators who were blinded to the experimental groups.

2.9. Hematoxylin and eosin (H&E) staining

An H&E staining kit was used for the observation of histological changes in brain tissue (Beyotime). Cortical brain sections (5 μm) were stained with hematoxylin and eosin according to the manufacturer's protocol. Images were visualized under a light microscope.

2.10. Nissl staining

Nissl staining was performed to reveal Nissl bodies using a Nissl staining solution (Beyotime) according to the manufacturer's instructions. Briefly, the sections were stained in Nissl staining solution for 5 min. After rinsing with distilled water, the slices were dehydrated and mounted with neutral balsam. Images were captured and analyzed using a light microscope.

2.11. Brain water content determination

Brain water content was used to assess cerebral edema as described elsewhere [22]. The brains were removed and placed on a dry surface. The cerebral hemisphere was equally cut along sagittal sutures. Samples were weighed using a chemical balance to acquire the wet weight, and then dried at 75 °C for 48 h obtain the dry weight. Brain water content was calculated as [(wet weight − dry weight) / wet weight] × 100%.

2.12. ELISA

The concentrations of TNF-α, IL-1β, IL-6, IL-18, CCL2 and CCL7 in the cortex and serum were measured with commercial ELISA kits (Jingmei Biotechnology).

Sample preparation: For the detection of brain protein levels, ipsilateral cortical tissues were rinsed with cold PBS to remove residual blood, weighted, and shredded. Then tissue samples were homogenized in ice-cold PBS (1:9, w/v) with protease inhibitor cocktail using pellet pestles on ice. The supernatants were collected after centrifugation at 5000 × *g* for 5–10 min. For the detection of serum protein levels, blood was collected from the apex of the heart and let sit at 4 °C for more than 30 min. The supernatants were collected after centrifugation at 3500 × *g* for 20 min.

Assay procedure: Briefly, 10 ul sample plus 40ul sample diluent were loaded into the wells and incubated at room temperature for 1 h. Then the plates were incubated with 50 μL antibody cocktail. After washing, plates were incubated with 50 μL of substrate A for 15 min, then 50 μL of solution B for another 15 min. The reaction was stopped by adding 50 μL of stop solution to each well. Absorbance was read at 450 nm. The values were compared to the standard curve, and the concentrations were determined.

2.13. Immunofluorescence staining

Immunofluorescence staining was performed as described elsewhere [23]. Briefly, cryosections or cells were post-fixed in 4% paraformaldehyde for 10 min, washed in PBS, and then permeabilized with 1% Triton® X-100/PBS for 10 min. Non-specific labeling was blocked by 10% goat serum for 1 h. For antigen detection, sections were incubated with anti-GFAP (Abcam, ab279290), anti-Iba-1 (Wako, 019–19741, 016–26721), or anti-CCL7 (Bioss, bs-1987R), anti-IL-1β (CST, 12242), and anti-CCR2 (Invitrogen, PA5-23043) at 4 °C overnight. The following day, sections were washed in PBS and incubated with goat anti-rabbit or anti-mouse IgG antibodies conjugated to AlexaFluor488 or AlexaFluor594 for 1 h at room temperature. Images were processed with Image J for quantification analysis.

2.14. Western blot

The western blot was conducted as previously described [24]. Total

a

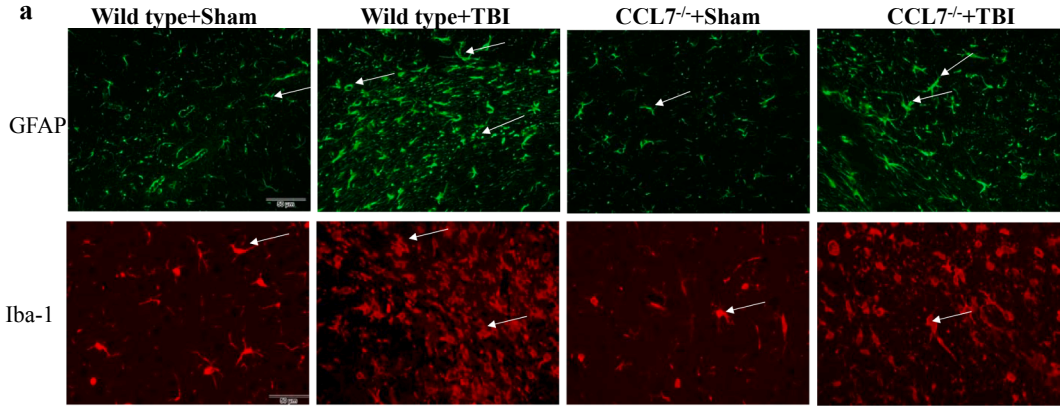

b

	Wild type+Sham	Wild type+TBI	CCL7$^{-/-}$+Sham	CCL7$^{-/-}$+TBI
GFAP$^+$cells/mm^2	917.0±43.10	1434±44.39$^{\#\#}$	956.0±24.83	1093±96.75$^{\&\&}$
Iba-1$^+$ cells/mm^2	132.3±8.950	388.0±10.41$^{\#\#}$	138.0±1.155	216.3±18.52$^{\&\&}$

c

		Wild type+Sham	Wild type+TBI	CCL7$^{-/-}$+Sham	CCL7$^{-/-}$+TBI
Cortex (pg/mg)	TNF-α	5.842±0.2474	11.34±0.7393$^{\#\#}$	6.602±0.3185	8.653±0.4328$^{\&}$
	IL-1β	3.075±0.3242	7.118±0.2832$^{\#\#}$	3.648±0.3369	5.545±0.3579$^{\&}$
	IL-6	15.19±0.7848	25.30±0.7947$^{\#\#}$	16.59±1.108	20.13±0.6713$^{\&\&}$
	IL-18	26.35±1.623	42.56±1.623$^{\#\#}$	30.77±1.824	34.39±1.304$^{\&}$
Serum (pg/mL)	TNF-α	52.91±4.731	124.8±9.759$^{\#\#}$	66.69±7.744	79.44±4.282$^{\&\&}$
	IL-1β	41.56±4.045	79.08±3.029$^{\#\#}$	42.86±1.282	59.51±2.767$^{\&\&}$
	IL-6	23.68±1.343	53.24±0.4960$^{\#\#}$	28.93±2.583	42.56±1.148$^{\&\&}$
	IL-18	35.88±1.838	63.82±1.871$^{\#\#}$	40.96±1.862	52.13±1.850$^{\&\&}$

Fig. 7. Effects of CCL7 deletion on TBI-induced inflammatory response. (a) Representative images of GFAP and Iba-1 immunoreactivities in the cortex of mice. Scale bar = 50 μm. (b) Quantification of GFAP$^+$ and Iba-1$^+$ cells per area (mm^2) in the cortex (n = 3 per group). (c) Concentrations of TNF-α, IL-1β, IL-6 and IL-18 in the cortex and serum were detected by ELISA kits. CCL7 knockdown attenuated TBI-induced increase in TNF-α, IL-1β, IL-6 and IL-18 levels (n = 6 per group). Data are presented as mean ± SEM. Statistical analysis: two-way ANOVA followed by Tukey correction. $^{\#\#}$ $p < 0.01$, compared to wild type + sham group; $^{\&}$ $p < 0.05$, $^{\&\&}$ $p < 0.01$, compared to wild type + TBI group.

protein was prepared by homogenizing the cortex and the concentration was determined by the bicinchoninic acid assay. Protein samples (2-3ul, 0.2–0.4ug/ul) were subjected to 15% SDS-Tris glycine gel electrophoresis and transferred to polyvinylidene-difluoride membranes. Subsequently, membranes were blocked with 3% BSA and incubated with polyclonal rabbit antibody raised against CCL7, CCL2 (CST, 41987) and CCR2 (Bioss, bs-10964R) overnight at 4 °C. An IgG monoclonal antibody against GAPDH was used as a loading control. The next morning, blots were washed in TBST and incubated with horseradish peroxidase conjugated anti-rabbit antibodies for 1.5 h at room temperature. The membrane was developed using the ECL-Plus protein detection kit. Signals were detected using chemiluminescence and analyzed by ImageJ software.

2.15. Real time RT-Pcr

Real-time RT-PCR analysis was performed using the SYBR Green PCR Master Mix and 7300 real-time PCR system as previously described [25]. GAPDH was used as an internal standard. The following oligonucleotides were used as primers:

Primers	Forward	Reverse
CCL7	5′-ACAAAAGATCCCCAAGAGGAAT-3′	5′-TCTTGAAGATAACAGCTTCCCA-3′
CCL2	5′-TTTTTGTCACCAAGCTCAAGAG-3′	5′-TTCTGATCTCATTTGGTTCCGA-3′
CCR2	5′-GCTCATCTTTGCCATCATGATT-3′	5′-TCATTCCAAGAGTCTCTGTCAC-3′
GAPDH	5′-AGGTCGGTGTGAACGGATTTG-3′	5′-TGTAGACCATGTAGTTGAGGTCA−3′

2.16. Statistical analysis

All data were expressed as means ± SEM. The data were statistically analyzed by one-way analysis of variance (ANOVA) with Dunnet correction or two-way ANOVA with Tukey correction using GraphPad Prism 8 software. $p < 0.05$ was considered statistically significant.

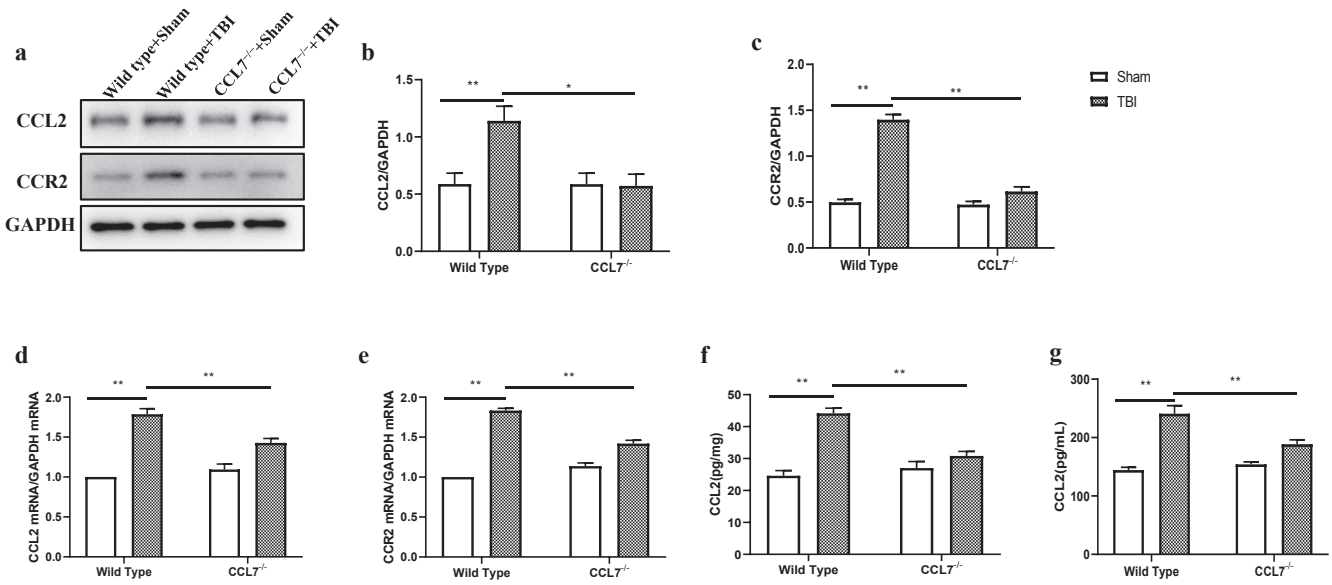

Fig. 8. Effects of CCL7 deletion on TBI-induced production of CCL2 and CCR2. (a-c) Western blots of CCL2 and CCR2 in cerebral cortex. Quantification of CCL2 and CCR2 protein abundance relative to GAPDH loading control (n = 3 per group). (d-e) mRNA levels of CCL2 and CCR2 in the cortex were assessed by real-time PCR (n = 3 per group). (f-g) CCL2 levels in the cortex of wild type and $CCL7^{-/-}$ mice were detected with ELISA (n = 6 per group). Data are presented as mean ± SEM. Statistical analysis: two-way ANOVA followed by Tukey correction. * $p < 0.05$, ** $p < 0.01$, compared to wild type + TBI group.

3. Results

3.1. TBI leads to neurological deficits and pathological changes

To assess neurological damage following TBI, a time course of behavioral tests including NOR, mNSS and OFT were carried out 24, 72 and 168 h post CCI surgery (Fig. 1). In the NOR test, mice underwent TBI showed significant lower discrimination index relative to the shams, demonstrating cognitive deficits following TBI. Moreover, TBI significantly elevated mNSS scores when compared with sham levels, suggesting declined neurological function. To examine spontaneous locomotor activity and anxiety-like behavior, mice were subject to the OFT test. TBI mice spent shorter time in the central area and traveled less total distance compared with the Sham group, reflecting that TBI elicited anxiety and harmed general locomotor activity.

The brains of the mice were examined postmortem. Fig. 2a shows representative images of the H&E-stained coronal section following TBI injury. Note that brain tissue in the sham group had clear brain tissue structure and regular cell arrangement. In contrast, heavy bleeding, irregular shape, eosinophil accumulation, nuclear pyknosis and increased glial cells were observed in the cortex on the lesion side. The neuronal survival in the *peri*-impact area of the cortex was investigated with Nissl staining (Fig. 2b-c). The TBI groups had a significantly lower percentage of neuronal survival than the sham animals. Next, we assessed blood–brain barrier (BBB) permeability using the brain water content measurement. The results demonstrated that CCI caused a significant increase in the ratio of water content in the injured cerebral hemisphere.

3.2. TBI triggers microglia-mediated inflammatory response

To assess whether TBI triggers microglia-mediated inflammation, the co-localization of Iba-1 (a marker for microglia) with IL-1β and CCR2, as well as the levels of pro-inflammatory cytokines and chemokines were determined. Our results demonstrated that TBI mice had increased co-localization of Iba-1 with IL-1β and CCR2 in the perilesional cortex tissue relative to the sham group (Fig. 3a-b). Moreover, enhanced circulating levels of TNF-α, IL-1β, IL-6 and IL-18 were observed in the serum and cortex obtained from TBI mice (Fig. 3c), as compared with sham controls. TBI also increased CCL2 concentrations in the cortex and serum (Fig. 4a). The mRNA and protein expression levels of CCL2 and CCR2 were elevated following TBI (Fig. 4b-d). All together, these findings suggest the microglia-controlled inflammatory response following TBI.

3.3. TBI upregulates astrocytes-derived CCL7 expression

We further examined astrocytes-released CCL7 expression by the co-localization of CCL7 and GFAP (a marker for astrocytes). The results showed mice that underwent TBI had significantly increased $GFAP^{+}$ cells as well as CCL7 co-localization with GFAP compared with controls (Fig. 5a), indicating the occurrence of reactive astrogliosis and the increase of astrocytes-derived CCL7 after TBI. Additionally, TBI promoted CCL7 production in the cortex and serum, and increased the mRNA and protein levels of CCL7 in the cortex (Fig. 5b-e).

3.4. CCL7 deletion attenuates neurological deficits and pathological changes after TBI

To investigate the role of CCL7 in TBI, $CCL7^{-/-}$ mice were used in this study. Behavioral tests showed that the increased mNSS score and decreased discrimination index, time spent in center and total distance travelled following CCI modeling were all reversed by CCL7 deletion (Fig. 6a). Furthermore, degenerated cells and brain edema were profoundly alleviated by CCL7 knockout (Fig. 6b-c). Together, these data indicated that CCL7 deletion attenuates the neurological defects and pathological changes after TBI.

3.5. CCL7 deletion reduces microglia-mediated inflammatory response after TBI

Next, we evaluated the involvement of CCL7 on microglia-mediated inflammation following TBI. Fig. 7 shows that the Iba-1 and GFAP immunoreactivity as well as TNF-α, IL-1β, IL-6 and IL-18 production in the cortex and serum were increased following TBI surgery, while were greatly decreased after CCL7 ablation. Consistent with these results, CCL7 knockout reversed the protein and mRNA expression of CCL2 and CCR2 in the cortex, and reduced CCL2 concentrations in the cortex and serum (Fig. 8). Taken together, these findings indicate that CCL7 plays a

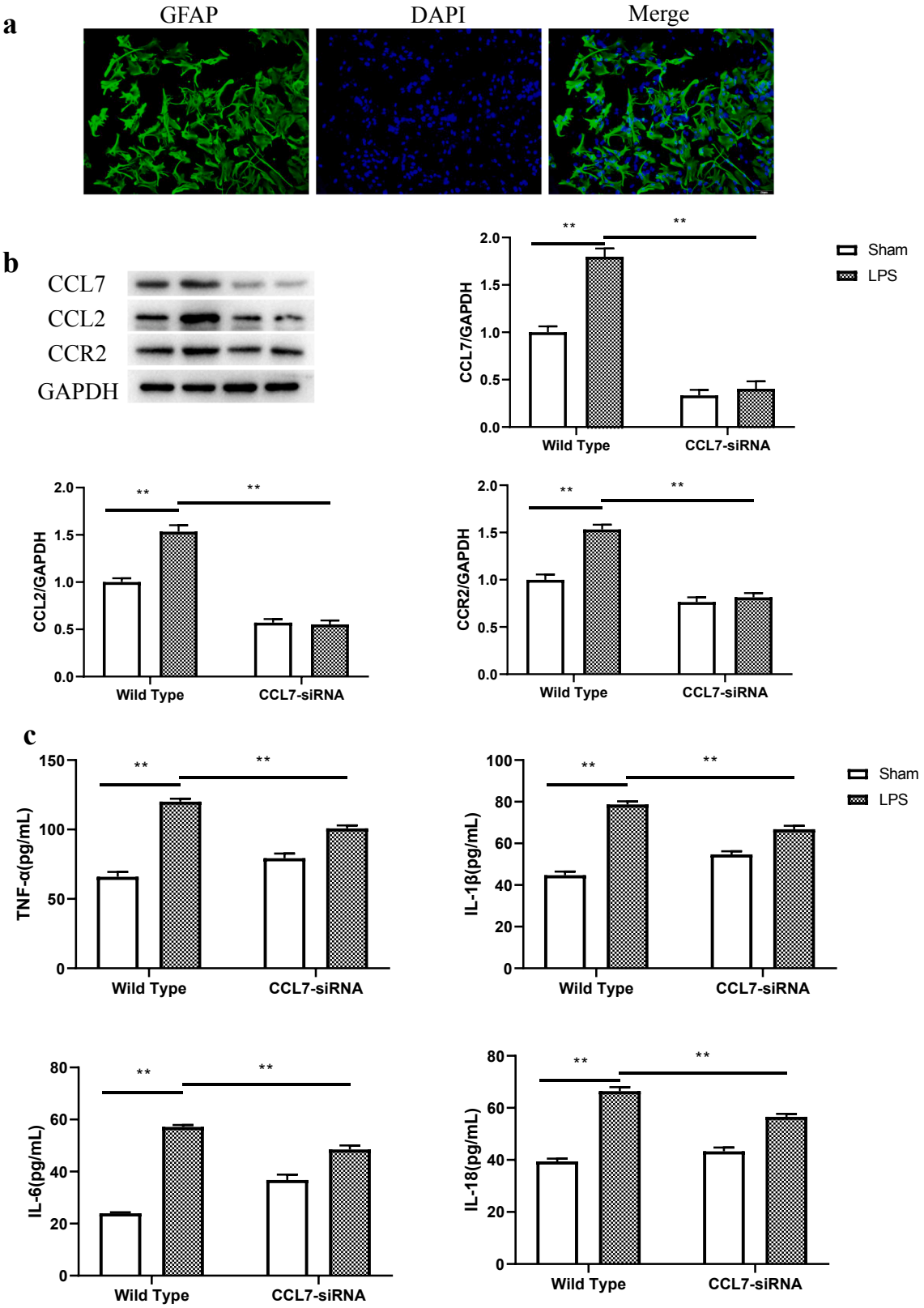

Fig. 9. Effect of CCL7 siRNA on LPS-stimulated co-culture of microglia and astrocytes. (a) Representative immunostaining staining of GFAP positive (primary astrocytes) cells counterstained with DAPI. Scale bar = 50 μm. (b) Representative images and quantitative analysis of CCL7, CCL2 and CCR2 expression in the co-culture of BV2 cells and primary astrocytes. (c) Concentration of inflammatory cytokines including TNF-α, IL-1β, IL-6 and IL-18 determined by ELISA. Data are presented as mean ± SEM. Statistical analysis: two-way ANOVA followed by Tukey correction. ** $p < 0.01$, compared to wild type + LPS group.

critical role TBI-triggered neuroinflammation.

3.6. CCL7 siRNA reversed LPS-stimulated inflammatory response in the co-culture of microglia and astrocytes.

To verify the effect of astrocyte-derived CCL7 on microglial activation in vitro, we co-culture primary astrocytes (Fig. 9a) with BV2 microglia cells. Primary astrocytes were transfected with CCL7 lentivirus for CCL7 inhibition, and then co-cultured with BV2 cells. LPS (a strong stimulator of microglial activation) was subsequently used to stimulate an inflammatory response in microglia [26]. The western blot analysis revealed that LPS treatment markedly upregulated the protein expression of CCL7, CCL2 and CCR2 in the co-culture, which was reversed in the presence of CCL7 siRNA (Fig. 9b). Moreover, protein analysis via ELISA showed a significant increase in the release of TNF-α, IL-1β, IL-6 and IL-18 following LPS intervention, which was also suppressed by CCL7-siRNA transfection (Fig. 9c). These results indicate that astrocyte-derived CCL7 facilitates microglial activation in vitro.

4. Discussion

Traumatic brain injury (TBI) is a common neural trauma caused by blunt mechanical force, and is considered as a critical public health and socioeconomic problem throughout the world [27]. TBI consists of a primary injury from the immediate mechanical insult and a secondary injury due to the pathology of blood brain barrier (BBB) disruption, excitotoxicity, neuronal cell death, inflammatory response, mitochondrial dysfunction and free radical formation. The second injury leads to a high mobility of long-term disability including PTSD, cognitive impairments, and neurobehavioral deficits [28,29].

Inflammation is the body's response to tissue damage, including infection, trauma, and disease [30]. The role of inflammation perpetuating the secondary injury response following traumatic brain injury has received a significant amount of attention over the last two decades as it dictates disease progression and impact post-injury recovery [31]. Microglia are specialized immune cells of the brain with phagocytic and antigen-presenting capabilities [7]. As the primary mediators of the innate immune response in the CNS, microglia are constantly surveying their environment for deleterious signals of foreign or endogenous origin [32]. Upon detection of an insult, microglia respond by becoming activated and initiate a neuroinflammatory response which, includes production of cytokines and chemokines, to recruit additional cells and induce them to clear injurious agents and maintain brain homeostasis [33]. However, recent evidence indicates that the homeostatic functioning of microglia is compromised in traumatic brain injury, results in a chronic neuroinflammatory state [31]. Johnson et al. examined the pathological changes in injured post-mortem human brains and demonstrated that a single moderate or severe TBI is associated with persistent activation of microglia (CR3/43- and/or CD68-immunoreactive) in the corpus callosum up to 18 years post injury [34]. Similarly, in a TBI mouse model, persistent microglial activation was observed in the injured cortex 1 year after CCI, and was associated with progressive lesion expansion, hippocampal neurodegeneration, myelin loss, activated neuroinflammation and oxidative stress [35]. Moreover, increased TNF-α concentration was observed in patients with traumatic brain injury [36]. TBI provoked microglia activation and upregulated the protein expressions of NF-κB, TNF-α, IL-1β, and IL-6 in the *peri*-contusive cortex of rats [37]. In line with these studies, we found that mice underwent CCI modeling had enhanced Iba-1^{+}IL-1β^{+} and Iba-1^{+}CCR2^{+} immunoreactivities and promoted TNF-α, IL-1β, IL-6, IL-18, CCL2 and CCR2 levels, confirming the activation of microglia-evoked inflammatory response following TBI.

CCL7 is one of the most pluripotent chemokines that plays a pivotal role in immune response [38]. CCL7 activation results in a significant enhancement in CCL20, IL-12p40 and IL-17C levels in a mouse model of psoriasis [12]. CCL7 deficiency attenuated LPS-induced total leukocyte and neutrophil accumulation in mice [39]. Astrocytes, the potent producers of CCL7, are characteristic star-shaped glial cells that participate in numerous aspects of central nervous system (CNS) physiology ranging from ion balance to metabolism [40]. A study showed that astrocytes-released CCL7 could activate spinal microglia by stimulating CCR2 (a CCL7 receptor that mainly detected in microglia) under the neuropathic pain [14]. In this study, TBI increased CCL7 co-localization with GFAP and upregulated CCR2 levels, demonstrating the interaction between astrocytes and microglia through CCL7 signaling in TBI. Furthermore, CCL7 deficiency mitigated microglia-controlled inflammatory response, brain morphology and neurological dysfunction after TBI, confirming the essential role of CCL7 in TBI-post recovery.

5. Conclusion

In summary, we have identified a critical role for astrocyte-derived CCL7 in microglia-controlled inflammatory response following TBI. These results also suggest that CCL7 could serve as a promising target for the treatment of TBI.

CRediT authorship contribution statement

Jianqin Xue: Conceptualization, Methodology, Supervision. **Yu Zhang:** Investigation, Methodology, Visualization. **Junhua Zhang:** Methodology, Validation, Writing – review & editing. **Zhujun Zhu:** Data curation, Formal analysis, Software. **Qi Lv:** Project administration, Resources, Writing – original draft. **Jianhua Su:** Conceptualization, Funding acquisition, Writing – review & editing.

Declaration of Competing Interest

The authors declare that they have no known competing financial interests or personal relationships that could have appeared to influence the work reported in this paper.

References

[1] F. Guan, T. Huang, X. Wang, Q. Xing, K. Gumpper, P. Li, J. Song, T. Tan, G.L. Yang, X. Zang, J. Zhang, Y. Wang, Y. Yang, Y. Liu, Y. Zhang, B. Yang, J. Ma, S. Ma, The TRIM protein Mitsugumin 53 enhances survival and therapeutic efficacy of stem cells in murine traumatic brain injury, Stem Cell Res Ther 10 (1) (2019) 352.
[2] X. Xiao, Y. Jiang, W. Liang, Y. Wang, S. Cao, H. Yan, L. Gao, L. Zhang, miR-212-5p attenuates ferroptotic neuronal death after traumatic brain injury by targeting Ptgs2, Mol Brain 12 (1) (2019) 78.
[3] G.B.D.N. Collaborators, Global, regional, and national burden of neurological disorders, 1990–2016: a systematic analysis for the Global Burden of Disease Study 2016, Lancet Neurol 18 (5) (2019) 459–480.
[4] K. Shi, J. Zhang, J.-F. Dong, F.-D. Shi, Dissemination of brain inflammation in traumatic brain injury, Cell Mol Immunol 16 (6) (2019) 523–530.
[5] R. Kuwar, A. Rolfe, L. Di, H. Xu, L. He, Y. Jiang, S. Zhang, D. Sun, A novel small molecular NLRP3 inflammasome inhibitor alleviates neuroinflammatory response following traumatic brain injury, J Neuroinflammation 16 (1) (2019) 81.
[6] X. Chen, S. Wu, C. Chen, B. Xie, Z. Fang, W. Hu, J. Chen, H. Fu, H. He, Omega-3 polyunsaturated fatty acid supplementation attenuates microglial-induced inflammation by inhibiting the HMGB1/TLR4/NF-kappaB pathway following experimental traumatic brain injury, J Neuroinflammation 14 (1) (2017) 143.
[7] I.P. Karve, J.M. Taylor, P.J. Crack, The contribution of astrocytes and microglia to traumatic brain injury, Br J Pharmacol 173 (4) (2016) 692–702.
[8] A. Kumar, B.A. Stoica, D.J. Loane, M. Yang, G. Abulwerdi, N. Khan, A. Kumar, S. R. Thom, A.I. Faden, Microglial-derived microparticles mediate neuroinflammation after traumatic brain injury, J Neuroinflammation 14 (1) (2017) 47.
[9] C.L. Sokol, A.D. Luster, The chemokine system in innate immunity, Cold Spring Harb Perspect Biol 7 (5) (2015) a016303, https://doi.org/10.1101/cshperspect.a016303.
[10] K. Zhang, J. Luo, Role of MCP-1 and CCR2 in alcohol neurotoxicity, Pharmacol Res 139 (2019) 360–366.
[11] J. Li, G. Deng, H. Wang, M. Yang, R. Yang, X. Li, X. Zhang, H. Yuan, Interleukin-1beta pre-treated bone marrow stromal cells alleviate neuropathic pain through CCL7-mediated inhibition of microglial activation in the spinal cord, Sci Rep 7 (2017) 42260.
[12] P.M. Brunner, E. Glitzner, B. Reininger, I. Klein, G. Stary, M. Mildner, P. Uhrin, M. Sibilia, G. Stingl, CCL7 contributes to the TNF-alpha-dependent inflammation of lesional psoriatic skin, Exp Dermatol 24 (7) (2015) 522–528.
[13] M.R. Freeman, Specification and morphogenesis of astrocytes, Science 330 (6005) (2010) 774–778.

[14] S. Imai, D. Ikegami, A. Yamashita, T. Shimizu, M. Narita, K. Niikura, M. Furuya, Y. Kobayashi, K. Miyashita, D. Okutsu, A. Kato, A. Nakamura, A. Araki, K. Omi, M. Nakamura, H. James Okano, H. Okano, T. Ando, H. Takeshima, T. Ushijima, N. Kuzumaki, T. Suzuki, M. Narita, Epigenetic transcriptional activation of monocyte chemotactic protein 3 contributes to long-lasting neuropathic pain, Brain 136 (3) (2013) 828–843.
[15] M. Zhang, W. Yang, P. Wang, Y. Deng, Y.T. Dong, F.F. Liu, R. Huang, P. Zhang, Y. Q. Duan, X.D. Liu, D. Lin, Q. Chu, B. Zhong, CCL7 recruits cDC1 to promote antitumor immunity and facilitate checkpoint immunotherapy to non-small cell lung cancer, Nat Commun 11 (1) (2020) 6119.
[16] T.J. Kramer, N. Hack, T.J. Bruhl, L. Menzel, R. Hummel, E.V. Griemert, M. Klein, S. C. Thal, T. Bopp, M.K.E. Schafer, Depletion of regulatory T cells increases T cell brain infiltration, reactive astrogliosis, and interferon-gamma gene expression in acute experimental traumatic brain injury, J Neuroinflammation 16 (1) (2019) 163.
[17] E.L. Ma, A.D. Smith, N. Desai, L. Cheung, M. Hanscom, B.A. Stoica, D.J. Loane, T. Shea-Donohue, A.I. Faden, Bidirectional brain-gut interactions and chronic pathological changes after traumatic brain injury in mice, Brain Behav Immun 66 (2017) 56–69.
[18] E.J. Lee, J.S. Park, Y.Y. Lee, D.Y. Kim, J.L. Kang, H.S. Kim, Anti-inflammatory and anti-oxidant mechanisms of an MMP-8 inhibitor in lipoteichoic acid-stimulated rat primary astrocytes: involvement of NF-kappaB, Nrf2, and PPAR-gamma signaling pathways, J Neuroinflammation 15 (1) (2018) 326.
[19] S.-I. Kano, E.Y. Choi, E. Dohi, S. Agarwal, D.J. Chang, A.M. Wilson, B.D. Lo, I.V. L. Rose, S. Gonzalez, T. Imai, A. Sawa, Glutathione S-transferases promote proinflammatory astrocyte-microglia communication during brain inflammation, Sci Signal 12 (569) (2019) eaar2124, https://doi.org/10.1126/scisignal.aar2124.
[20] A.C. Kaufman, S.V. Salazar, L.T. Haas, J. Yang, M.A. Kostylev, A.T. Jeng, S. A. Robinson, E.C. Gunther, C.H. van Dyck, H.B. Nygaard, S.M. Strittmatter, Fyn inhibition rescues established memory and synapse loss in Alzheimer mice, Ann Neurol 77 (6) (2015) 953–971.
[21] J. Chen, P.R. Sanberg, Y. Li, L. Wang, M. Lu, A.E. Willing, J. Sanchez-Ramos, M. Chopp, Intravenous administration of human umbilical cord blood reduces behavioral deficits after stroke in rats, Stroke 32 (11) (2001) 2682–2688.
[22] X. Jin, T. Wang, Y. Liao, J. Guo, G. Wang, F. Zhao, Y. Jin, Neuroinflammatory Reactions in the Brain of 1,2-DCE-Intoxicated Mice during Brain Edema, Cells 8 (9) (2019) 987, https://doi.org/10.3390/cells8090987.
[23] A.P. Kann, R.S. Krauss, Multiplexed RNAscope and immunofluorescence on whole-mount skeletal myofibers and their associated stem cells, Development 146 (20) (2019).
[24] T.H. Huang, Y.W. Lin, C.P. Huang, J.M. Chen, C.L. Hsieh, Short-term auricular electrical stimulation rapidly elevated cortical blood flow and promoted the expression of nicotinic acetylcholine receptor alpha4 in the 2 vessel occlusion rats model, J Biomed Sci 26 (1) (2019) 36.
[25] M. Kato, J. Zhang, M. Wang, L. Lanting, H. Yuan, J.J. Rossi, R. Natarajan, MicroRNA-192 in diabetic kidney glomeruli and its function in TGF-beta-induced collagen expression via inhibition of E-box repressors, Proc Natl Acad Sci U S A 104 (9) (2007) 3432–3437.
[26] H.Y. Nam, J.H. Nam, G. Yoon, J.Y. Lee, Y. Nam, H.J. Kang, H.J. Cho, J. Kim, H. S. Hoe, Ibrutinib suppresses LPS-induced neuroinflammatory responses in BV2 microglial cells and wild-type mice, J Neuroinflammation 15 (1) (2018) 271.
[27] W. Liu, Y. Chen, J. Meng, M. Wu, F. Bi, C. Chang, H. Li, L. Zhang, Ablation of caspase-1 protects against TBI-induced pyroptosis in vitro and in vivo, J Neuroinflammation 15 (1) (2018) 48.
[28] Y.-L. Liu, Z.-M. Xu, G.-Y. Yang, D.-x. Yang, J. Ding, H. Chen, F. Yuan, H.-l. Tian, Sesamin alleviates blood-brain barrier disruption in mice with experimental traumatic brain injury, Acta Pharmacol Sin 38 (11) (2017) 1445–1455.
[29] H. Yang, Z.-T. Gu, L.i. Li, M. Maegele, B.-Y. Zhou, F. Li, M. Zhao, K.-S. Zhao, SIRT1 plays a neuroprotective role in traumatic brain injury in rats via inhibiting the p38 MAPK pathway, Acta Pharmacol Sin 38 (2) (2017) 168–181.
[30] C.K. Glass, K. Saijo, B. Winner, M.C. Marchetto, F.H. Gage, Mechanisms underlying inflammation in neurodegeneration, Cell 140 (6) (2010) 918–934.
[31] F. Corrigan, K.A. Mander, A.V. Leonard, R. Vink, Neurogenic inflammation after traumatic brain injury and its potentiation of classical inflammation, J Neuroinflammation 13 (1) (2016) 264.
[32] J.A. Rodríguez-Gómez, E. Kavanagh, P. Engskog-Vlachos, M.K.R. Engskog, A. J. Herrera, A.M. Espinosa-Oliva, B. Joseph, N. Hajji, J.L. Venero, M.A. Burguillos, Microglia: Agents of the CNS Pro-Inflammatory Response, Cells 9 (7) (2020) 1717, https://doi.org/10.3390/cells9071717.
[33] S. Hickman, S. Izzy, P. Sen, L. Morsett, J. El Khoury, Microglia in neurodegeneration, Nat Neurosci 21 (10) (2018) 1359–1369.
[34] V.E. Johnson, J.E. Stewart, F.D. Begbie, J.Q. Trojanowski, D.H. Smith, W. Stewart, Inflammation and white matter degeneration persist for years after a single traumatic brain injury, Brain 136 (Pt 1) (2013) 28–42.
[35] D.J. Loane, A. Kumar, B.A. Stoica, R. Cabatbat, A.I. Faden, Progressive neurodegeneration after experimental brain trauma: association with chronic microglial activation, J Neuropathol Exp Neurol 73 (1) (2014) 14–29.
[36] A.R. Crespo, A.B. Da Rocha, G.P. Jotz, R.F. Schneider, I. Grivicich, K. Pinheiro, C. Zanoni, A. Regner, Increased serum sFas and TNFalpha following isolated severe head injury in males, Brain Inj 21(4) (2007) 441-7.
[37] L. Tao, D. Li, H. Liu, F. Jiang, Y. Xu, Y. Cao, R. Gao, G. Chen, Neuroprotective effects of metformin on traumatic brain injury in rats associated with NF-kappaB and MAPK signaling pathway, Brain Res Bull 140 (2018) 154–161.
[38] S. Han, T. Wang, Y. Chen, Z. Han, L. Guo, Z. Wu, W. Yan, H. Wei, T. Liu, J. Zhao, W. Zhou, X. Yang, J. Xiao, High CCL7 expression is associated with migration, invasion and bone metastasis of non-small cell lung cancer cells, Am J Transl Res 11 (1) (2019) 442–452.
[39] P.F. Mercer, A.E. Williams, C.J. Scotton, R.J. Jose, M. Sulikowski, J.D. Moffatt, L.A. Murray, R.C. Chambers, Proteinase-activated receptor-1, CCL2, and CCL7 regulate acute neutrophilic lung inflammation, Am J Respir Cell Mol Biol 50(1) (2014) 144-57.
[40] J. Cohen, C. Torres, Astrocyte senescence: Evidence and significance, Aging Cell 18 (3) (2019) e12937, https://doi.org/10.1111/acel.2019.18.issue-310.1111/acel.12937.